Development of a combi-electrosensor for the detection of phenol by combining photoelectrochemistry and square wave voltammetry

Development of a Combi-Electrosensor for the Detection of Phenol by Combining Photoelectrochemistry and Square Wave Voltammetry

Liselotte Neven[1,2,‡], Hanan Barich[1,2,‡], Nick Sleegers[1,2], Rocío Cánovas[1,2], Gianni Debruyne[1] and Karolien De Wael*[1,2]

[1]*A-Sense Lab, Bioscience Engineering Department, University of Antwerp, Groenenborgerlaan 171, 2020 Antwerp, Belgium*

[2] *NANOlab Center of Excellence, University of Antwerp, Groenenborgerlaan 171, 2020 Antwerp, Belgium.*

‡ *Shared first author*

* *Corresponding author, e-mail: karolien.dewael@uantwerpen.be*

Abstract

The high toxicity, endocrine-disrupting effects and low (bio)degradability commonly attributed to phenolic compounds have promoted their recognition as priority toxic pollutants. For this reason, the monitoring of these compounds in industrial, domestic and agricultural streams is crucial to prevent and decrease their toxicity in our daily life. To confront this relevant environmental issue, we propose the use of a combi-electrosensor which combines singlet oxygen ($^1O_2$)-based photoelectrochemistry (PEC) with square wave voltammetry (SWV). The high sensitivity of the PEC sensor (being a faster alternative for traditional chemical oxygen demand–COD–measurements) ensures the detection of nmol L^{-1} levels of phenolic compounds while the SWV measurements (being faster than the color test kits) allow the differentiation between phenolic compounds. Herein, we report on the development of such a combi-electrosensor for the sensitive and selective detection of phenol (PHOH) in the presence of related phenolic compounds such as hydroquinone (HQ), bisphenol A (BPA), resorcinol (RC) and catechol (CC). The PEC sensor was able to determine the concentration of PHOH in spiked river samples containing only PHOH with a recovery between 96% and 111%. The SWV measurements elucidated the presence of PHOH, HQ and CC in the spiked samples containing multiple phenol compounds. Finally, the practicality of the combi-electrosensor set-up with a dual SPE containing two working electrodes and shared reference and counter electrodes was demonstrated. As a result, the combination of the two techniques is a powerful and valuable tool in the analysis of phenolic samples, since each technique improves the general performance by overcoming the inherent drawbacks that they display independently.

Keywords: Photoelectrochemistry, Square Wave Voltammetry, Dual Screen-Printed Carbon Electrode, Phenolic Compounds.

Introduction

Phenol (PHOH), which is mostly produced via the cumene hydroperoxide route,[1] is used in various production processes such as disinfectants, plasticizers, surfactants and pesticides.[2, 3] The growing amount of phenolic contamination in wastewater[4] leads to an increased level of detrimental effects on human and wildlife[5] due to their high toxicity,[6, 7] endocrine-disrupting effects[2, 8] and low (bio)degradability.[9] For this reason, phenolic compounds are recognized as priority toxic pollutants by different regulatory entities such as the Environmental Protection Agency of the United States (USEPA) and the European Commission (EC).[10] As a result, it is imperative to develop techniques for the monitoring of these phenols in the environment such as rivers, streams and industrial wastewaters.

The monitoring of phenolic compounds in wastewater is challenging due to the complex composition of industrial, domestic and agricultural streams.[11] Traditional methods include gas chromatography (GC) or liquid chromatography (LC) coupled with various detection techniques such as mass spectrometry (MS),[12-18] UV detection,[19-22] diode array detector (DAD)[16, 20, 23] and others.[16, 24] These are powerful techniques in terms of identification and quantification, possessing high sensitivity and accuracy. Nonetheless, their applicability on-site remains challenging due to the necessity of derivatization steps (for GC), expensive equipment, high measurement time and cost, and the need for trained personnel.[25-27] Furthermore, a pre-concentration and isolation step of the phenolic compounds by solid phase[12, 14, 17] or liquid-liquid[21-23] (micro)extraction are often a prerequisite in these detection methods.

The use of electrochemical (bio)sensors has emerged as a suitable alternative, complementary technique due to their ease in operation, fast response, low cost and low measuring volume. On-site detection can be performed by employing screen-printed electrodes (SPEs) with wireless potentiostats which are coupled to smartphones or laptops.[26-28] Moreover, the efficiency in oxidizing phenolic compounds makes electrochemistry an ideal detection method. Techniques such as cyclic voltammetry (CV),[29, 30] square wave voltammetry (SWV),[29, 31, 32] differential pulse voltammetry (DPV)[29, 33, 34] or amperometry[35, 36] have often been used for this purpose. Despite the aforementioned advantages, these strategies also face challenges such as the deactivation of electrodes due to the polymerization of phenoxy radicals on their surface upon multiple measurement cycles.[37, 38] This fouling phenomenon can be avoided by using single-use bare SPEs or modified SPEs with nanomaterials (e.g. carbon nanotubes).[28]

On the other hand, the modification of electrodes by enzymes promotes an improvement of the sensor's sensitivity with detection limits (LOD) in the μmol L^{-1} to nmol L^{-1} range.[39] Enzymes such as horseradish peroxidase (HRP),[40-42] tyrosinase[43, 44] and laccase[39] are often employed to accomplish a better sensitivity. Yet, thermal and chemical instability of the enzyme, reproducibility issues and the use of reagents, such as hydrogen peroxide (H_2O_2) in the case of HRP, limit their applicability in real scenarios.[45]

To maintain a low LOD but overcome the drawbacks linked to the use of enzymes, new enzyme-inspired catalytic strategies have been pursued.[45, 46] Trashin *et al.*[45] developed a highly sensitive photoelectrochemical (PEC) approach which uses a photosensitizer (PS) type II to aerobically produce singlet oxygen ($^1O_2$) upon red light illumination. The produced $^1O_2$ oxidizes the phenolic compounds present in the sample and the following reduction at the electrode surface completes the electrocatalytic redox cycle. This PEC sensor can measure phenolic compounds in the low nmol L^{-1} range[45, 46] and easily intercept additional low concentration compounds by the increase of the total phenol photoresponse. However, due to the intrinsic properties of the sensor, identification of individual phenolic structures is impossible since all phenolics can contribute to the photocurrent. Indeed, the PEC sensor will indicate the total phenolic concentration, similar to the values obtained by a COD measurement. However, the COD method measures all oxidizable compounds and is, as a result, not specific for phenolic structures only. Moreover, a long digestion time for the COD limits its applicability on-site, in contrast to the much faster PEC sensor.[47]

The identification limitation of the PEC sensor can be overcome by introducing another electrochemical technique in parallel, i.e. SWV. The total concentration of the phenolic compounds is monitored by the PEC sensor while the identification of the different compounds contributing to the photoresponse occurs via the SWV measurement based on their oxidation potential.[48]

In this article, we demonstrate the synergic contribution between the PEC and SWV sensors emerging as a powerful tool for the simultaneous quantification and identification of phenolic samples. First, the optimization of the analytical parameters for the detection of PHOH will be described, together with interference studies in the presence of phenolic analogues, for each technique. The studied phenols include hydroquinone (HQ), bisphenol A (BPA), catechol (CC), resorcinol (RC) and *p*-benzoquinone (*p*-BQ) as example toxic compounds,[49, 50] possible oxidation products of PHOH[29] or side products of the cumene process for synthesizing PHOH.[51] Second, the two techniques (PEC and SWV) will be applied for the detection of PHOH in spiked river samples.

Lastly, the sensors will be combined into a combi-electrosensor which will be tested via the use of a SPE consisting of two working electrodes, one electrode modified for PEC sensing and the second electrode left unmodified to allow SWV sensing.

Experimental

Reagents

The perfluorophthalocyanine zinc complex, $F_{64}PcZn$, was synthesized and deposited on a TiO_2 P25 matrix, as described in previous work.[45] The final loading was 3wt%. The supported PS was abbreviated by $F_{64}PcZn|TiO_2$.

PHOH (99% purity), *p*-BQ (99% purity), CC (99% purity) and RC (99% purity) were purchased from J&K Scientific. HQ (99.5% purity) and BPA (99+% purity) were purchased from Acros Organics and Sigma Aldrich respectively. The phenolic compounds were dissolved in absolute ethanol (Fisher Chemical) and stored in an ice box.

Acetone, used for the leaching experiments, was purchased from VWR.

Sodium phosphates and sodium carbonates were obtained from Sigma-Aldrich and VWR, respectively. Sodium citrate, citric acid, borax ($Na_2B_4O_7 \cdot 10H_2O$) and boric acid were purchased from Merck. Potassium chloride and potassium hydroxide were obtained from Acros Organics.

Photoelectrochemical Sensing

Graphite SPEs were purchased from Metrohm DropSens. The pseudo-reference electrode (RE) was silver and the counter electrode (CE) and working electrode (WE) (Ø = 4 mm) consisted of graphite. The WE was coated with 3wt% $F_{64}PcZn|TiO_2$ by casting a small droplet of 5 µL from a 10 mg mL^{-1} aqueous suspension of $F_{64}PcZn|TiO_2$. The droplet was left to dry overnight resulting in a $F_{64}PcZn|TiO_2$-coated SPE.

Photoelectrochemical measurements were carried out on a µAutolab III (Metrohm Autolab) instrument with NOVA software. The measurements were conducted in an 80 µL droplet containing buffer solution with or without PHOH for, respectively, PHOH or blank measurement. No purging of the droplet with O_2 gas occurred. The level of O_2 in the droplet was in equilibrium with the O_2 in the lab environment. The potential of the silver (Ag) pseudo-reference electrode of the SPE was +0.05 V *vs.* SCE.

An illumination source, a diode laser operating at 655 nm, from Roithner Lasertechnik was used. The power was set to 0.24 W cm^{-2} and the laser was turned on and off at specific time intervals. The first illumination was used to adjust the laser beam focus to fully cover the WE surface of the SPE. This position was then fixed throughout the whole experiment.

A buffer solution, 0.02 mol L^{-1} phosphate buffer (KH_2PO_4) was used for pH-values between 6 and 8. For pH-values 9 and 10, 0.02 mol L^{-1} borate buffer (H_3BO_3) was used. Concentrated KOH solution was added dropwise to the buffer solutions until the desired pH-value was obtained, measured via a Metrohm pH-meter. In all buffer solutions, 0.1 mol L^{-1} KCl was present as a supporting electrolyte.

Linear sweep voltammetry (LSV) measurements were performed to estimate the optimal potential window for the amperometric detection of PHOH. A conditioning step was first carried out at 0.10 V for 5 s. Then, the potential was scanned from 0.10 V to −0.25 V *vs.* Ag pseudo-reference electrode with a step potential of 1.00 mV and a scan rate of 0.25 mV s^{-1}. The laser was consecutively switched on and off for 30 s. The LSV measurements were taken at several pH-values.

The optimal measurement condition for the amperometric detection of PHOH was −0.14 V *vs*. Ag pseudo-reference in pH 9 borate buffer. The laser was programmed to switch on for 20 s and off for 40 s to restore the baseline current to its initial value. The LOD was determined by 3 times the standard deviation of the blank divided by the slope of the calibration plot. The limit of quantification (LOQ) was calculated by the standard deviation of the blank multiplied by 10 divided by the slope of the calibration plot.

Square Wave Voltammetry

Disposable ItalSens IS-C graphite SPEs were purchased from PalmSens. The pseudo-RE was silver and the CE and WE consisted of graphite (Ø = 3 mm). The SWV measurements were performed on a MultiPalmSens4 or EmStat Blue potentiostats (PalmSens, The Netherlands) with PSTrace/MultiTrace or PStouch software, respectively. The measurements were conducted in an 80 µL droplet. The potential of the Ag pseudo-reference electrode of the SPE was +0.05 V *vs.* SCE.

As buffer solution, different phosphate buffers were used: i) 0.02 mol L^{-1} H_3PO_4/NaH_2PO_4 for pH 2; ii) 0.02 mol L^{-1} Na_2HPO_4/NaH_2PO_4 for pH-values 6 and 8; and iii) 0.02 mol L^{-1} NaH_2PO_4/ Na_3PO_4 for pH 12. For pH 4, 0.02 mol L^{-1} citric acid/sodium citrate buffer was used,

and carbonate buffer, 0.02 mol L^{-1} $NaHCO_3/Na_2CO_3$, was used for pH 10. Adjustment of the pH-value, measured with a Metrohm pH-meter, was obtained by adding 0.1 mol L^{-1} KOH solution. In all buffer solutions, 0.1 mol L^{-1} KCl was present as supporting electrolyte.

For the optimal detection of phenols by SWV, a potential scan range of −0.3 V to 1.1 V (vs Ag pseudo-reference electrode) with a frequency of 10 Hz, amplitude of 25 mV and step potential of 5 mV was applied. The SWV measurements were taken at several pH-values. All voltammograms were background corrected using the "moving average iterative background correction" (peak width = 1) tool in the PSTrace software. The optimal buffer for SWV detection of PHOH was pH 10 carbonate buffer. The LOD and LOQ were determined according to the calculation as described in section 'Photoelectrochemical Sensing'.

Measurements with the combi-electrosensor (PEC and SWV)

To combine PEC and SWV in one measurement, electrode strips with two WEs (Metrohm Dropsens SPE Dual Screen-Printed Carbon Electrode Ref. X1110 displayed in the Figure 1.A) were used. One of the WEs was modified with $F_{64}PcZn|TiO_2$ to allow the PEC measurements. The second WE was left unmodified for SWV analysis. The measurements were conducted on a PalmSens bipotentiostat using the PSTrace software. The SPE consisted of a Ag RE, graphite CE and two graphite WEs. The measurements were conducted in a 120 µL droplet of 10 µmol L^{-1} PHOH covering both WEs, CE and RE. pH 8, 9 and 10 buffer solutions were all tested.

Prior to the measurement, one WE was coated with 3wt% $F_{64}PcZn|TiO_2$ according to the procedure described in the 'Photoelectrochemical Sensing' section. The droplet volume of the 10 mg mL^{-1} aqueous $F_{64}PcZn|TiO_2$ suspension used was 2.5 µL instead of 5.0 µL due to the smaller size of the WE. For the PEC measurements, a potential of −0.14 V *vs.* Ag pseudo-reference electrode was applied. The laser (655 nm, 0.24 W cm^{-2}) was manually switched on and off at specific time intervals.

The parameters of the SWV measurements used were a potential range from −0.3 V to 1.1 V *vs.* Ag pseudo-reference electrode, frequency of 10 Hz, 25 mV amplitude and 5 mV step potential.

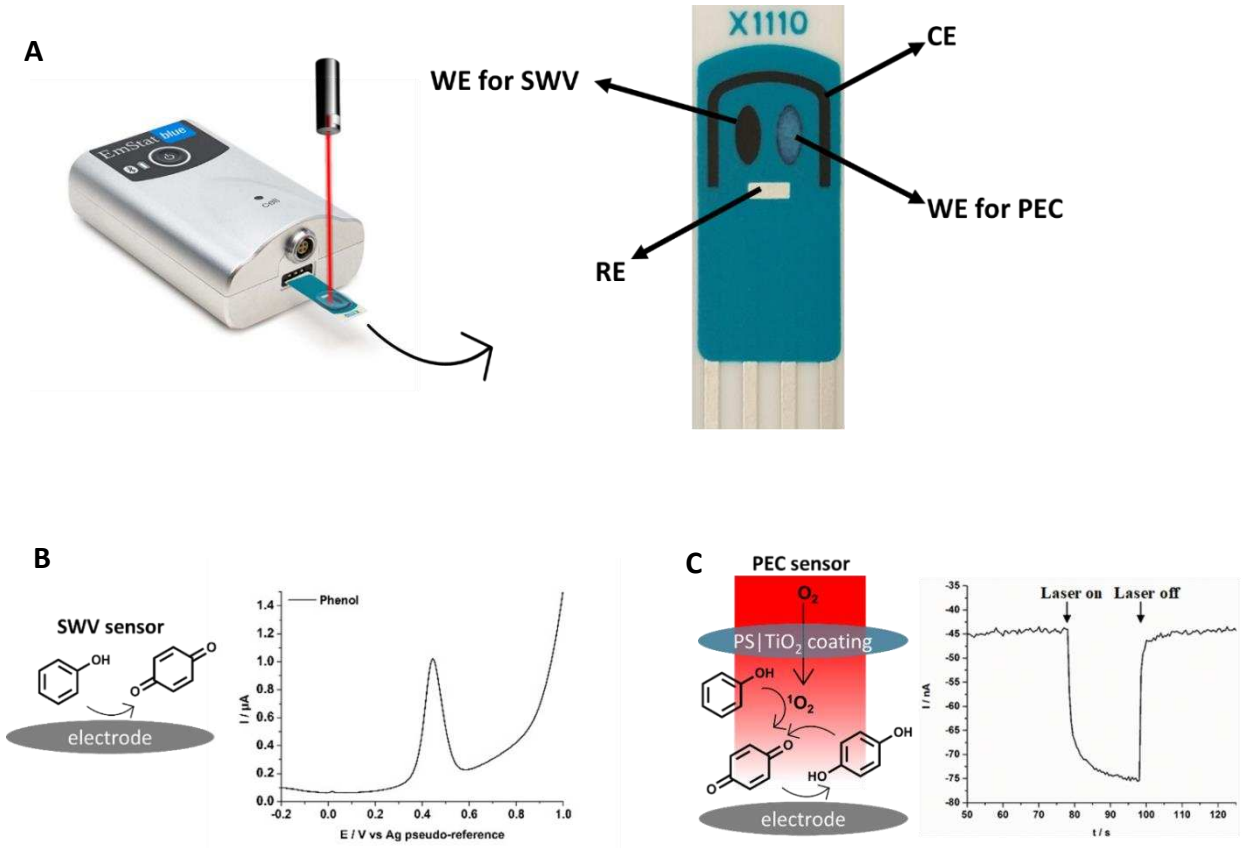

Figure 1. *Dual SPE, integrated in a wireless portable potentiostat, with two WEs used for the combi-electrosensor (A). Left WE is bare graphite and right is a $F_{64}PcZn|TiO_2$-coated graphite WE. Schematic representation of the square wave voltammetric (SWV) detection (i.e. oxidation of phenols by the application of increasing oxidative potentials) (B) and photoelectrochemical (PEC) sensing mechanism (C) based on $^1O_2$ being formed upon illumination by a 655 nm laser of a type II PS ($F_{64}PcZn|TiO_2$). Its $^1O_2$ production leads to the oxidation of phenolic compounds. The subsequent reduction of the oxidized phenolic compounds at the electrode completes the electrocatalytic redox cycle and leads to a photocurrent response under illumination.*

Measurements in real samples

River samples were collected from the Stiemer (Diepenbeek, Belgium), Albert Canal (Genk, Belgium) and the Scheldt (Antwerp, Belgium). These samples were filtered, to remove micro-floats which can potentially block the illumination of the electrode surface by the laser in the PEC sensor, and equilibrated at room temperature prior to the measurements to remove the influence of the temperature on the measurements. The river samples were spiked with PHOH by diluting the PHOH stock solution, made in ethanol, with the river samples until 5.0 µmol L^{-1}

PHOH was obtained. Different samples A-E were made. Samples A, B and C consisted of Stiemer, Scheldt and Albert Canal river samples, respectively, spiked with 5.0 µmol L^{-1} PHOH. Sample D contained an Albert Canal river sample with 5.0 µmol L^{-1} PHOH and 2.5 µmol L^{-1} HQ. Sample E consisted of an Albert Canal river sample containing 5.0 µmol L^{-1} PHOH, 2.5 µmol L^{-1} HQ and 10 µmol L^{-1} CC.

The standard addition method was carried out in the optimal measurement conditions by the PEC sensor by adding a standard PHOH solution in buffer to the diluted spiked river samples. The spiked river samples were diluted 25 times with pH 9 borate buffer so that the standard addition could be performed in the linear dynamic range of PHOH. For the SWV measurements, the spiked river samples were diluted 6.7 times with pH 10 carbonate buffer.

Leaching experiment of $F_{64}PcZn|TiO_2$ with acetone

Leaching experiments with acetone were conducted with the PEC sensor to evaluate the influence of the organic solvent on the solubility of $F_{64}PcZn$ and the robustness of the $F_{64}PcZn|TiO_2$-coating on the SPE in general. The electrode surface was washed five times with the washing solution containing a mixture of acetone and Milli Q water. Several washing solutions were prepared, each with a higher percentage, ranging from 0 to 100% acetone in Milli Q water. Afterwards, the electrode surface was rinsed with Milli Q water to remove any residual acetone traces. The photoresponse of 10 µmol L^{-1} PHOH in pH 7 phosphate buffer (at −0.1 V *vs.* Ag pseudo-reference electrode) was recorded to evaluate the condition of the SPE-coating after the washing step. The obtained photosignals were plotted against the acetone percentage in the washing solution to determine the effects of washing $F_{64}PcZn|TiO_2$-coating on the analytical performance of the PEC sensor. For each washing solution, a novel $F_{64}PcZn|TiO_2$-coated SPE was used and the blanks (phosphate buffer pH 7) were measured to evaluate the initial condition of the $F_{64}PcZn|TiO_2$-coating and the quality of the SPE electrode.

Results and discussion

Sensitive PEC sensing of phenolic compounds

PEC sensing of PHOH. The PEC sensing mechanism is based on $^1O_2$ being formed upon illumination of a $F_{64}PcZn|TiO_2$-coated SPE (Figure 1.C). The oxidation of PHOH by $^1O_2$ results in

the formation of *p*-BQ via a [4 + 2]cycloaddition.[52] By applying a reductive potential at the electrode surface (e.g. −0.14 V *vs.* Ag pseudo-reference), *p*-BQ is reduced to HQ.[53] The latter compound can be oxidized further by $^1O_2$, producing *p*-BQ[45] and, thereby, establishing an electrocatalytic redox cycle.

Such an electrocatalytic redox cycle is established using chronoamperometry and photo-illumination. Figure 2 provides a typical current-time response for a $F_{64}PcZn|TiO_2$-coated SPE. During the first 5 s of illumination, the redox cycle is initiated and the reduction photocurrent increases (see Figure 2). This increase in reduction current can be explained by the fact that HQ has an oxidation rate by $^1O_2$ 15× greater than for PHOH.[54] During the last 15 s, the reduction current plateaus. This apparent stabilization occurs due to the continuous redox cycling effect involving the oxidation of HQ by $^1O_2$ and reduction of *p*-BQ to HQ. When illumination stopped, the current returns to its baseline value (approximately −45 nA) as the production of $^1O_2$, which maintains the photocurrent, ceases.

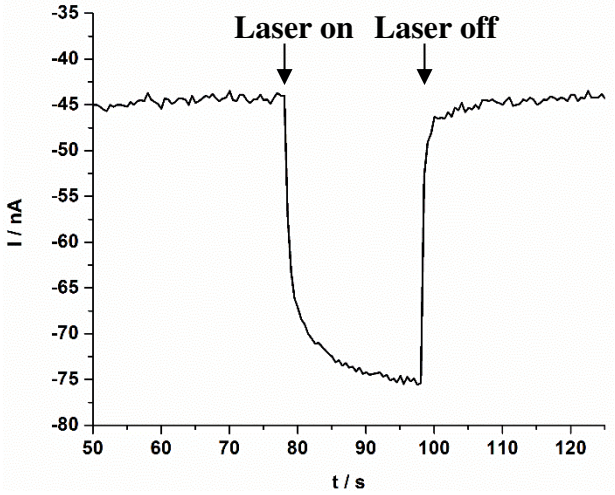

Figure 2. *Chronoamperometric measurement for a $F_{64}PcZn|TiO_2$-modified SP at −0.14 V vs. Ag pseudo-reference in 0.5 µmol L^{-1} PHOH in pH 9 buffer, illuminated for 20 s with red light (655 nm, 0.24 W cm^{-2}).*

In general, the sensitivity of the PEC sensor is affected by oxygenation kinetics, diffusion rates and reduction kinetics of the oxidized species. Optimizing one of these parameters can lead to an increase in the photoresponse. The enhancement of the diffusion of species towards the

electrode surface is a challenging process, but an efficient way to achieve this involves an incubation step where the compound is accumulated near the surface.[55] Such a method mostly works with large phenolic compounds with low solubility in water such as rifampicin;[56] yet smaller compounds such HQ do not incubate at the surface as they are easily removed by washing the surface.

The two remaining parameters, oxygenation and reduction kinetics, can be improved by careful selection of the applied reductive potential and the buffer pH. Therefore, the PEC detection of PHOH was first optimized with regards to applied potential and buffer pH by using a previously described protocol.[46]

Determination of the optimal potential window for PHOH detection via chopped LSV. Firstly, LSV measurements were recorded in pH 7 and pH 9 buffer solutions to determine the optimal potential windows for PHOH sensing (see Figure 3).[46] The laser was switched on and off at 30 s time intervals to reveal the baseline current and stable PHOH response. Due to the electrocatalytic redox cycle of PHOH, a response (dotted red line) considerably larger compared to that of the buffer (black line) was obtained. This latter current was caused by the reduction of $^1O_2$ produced in the vicinity of the electrode surface.[45]

The optimal potential window for PHOH detection was selected based on the ratio of the photocurrent response of PHOH and the buffer solution, where the phenol's response should be maximized compared to the buffer alone. This ratio is an indication of the sensitivity of the PEC measurement. At pH 7, a potential window was selected between −0.08 V to −0.13 V *vs*. Ag pseudo-reference (see Figure 3.A). Applying more negative reductive potentials results in increased photoresponse of the buffer solution whilst applying smaller negative reductive potentials decreases the response of PHOH.

The increment of the buffer to pH 9 (see Figure 3.B) not only improved the response of PHOH but also shifted the optimal potential window towards more reductive potentials. The reduction of *p*-BQ to HQ involves protons and is more facile at lower pH levels,[53] hence the negative shift in optimal potential window from −0.08 V to −0.13 V for pH 7 to −0.13 V to −0.18 V *vs.* Ag pseudo-reference electrode for pH 9.

Based on these optimal potential windows for pH 7 (−0.08 V to −0.13 V) and pH 9 (−0.13 V to −0.18 V), three potentials, i.e. −0.10 V and −0.14 V for pH 6 – 8 and −0.14 V and

−0.17 V for pH 9, were selected for the amperometric measurement to determine the optimal applied potential for the detection of PHOH.

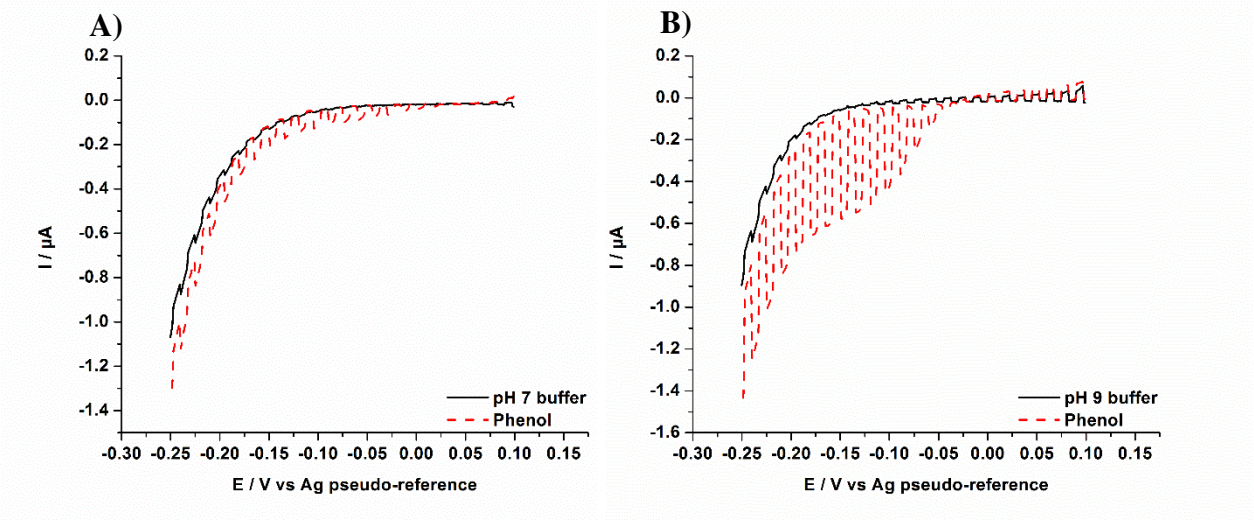

Figure 3. *Linear sweep voltammograms of buffer and buffer with 10 µmol L^{-1} PHOH recorded in (A) pH 7 and (B) pH 9. The scan rate and step potential were 0.25 mV s^{-1} and 1 mV. The laser (655 nm, 0.24 W cm^{-2}) was switched on and off at 30 s time intervals.*

Selection of optimal pH and applied potential for PHOH detection via amperometry. After the above first LSV screening, −0.10 V, −0.14 V and −0.17 V *vs.* Ag pseudo reference were chosen for amperometric measurements in buffers ranging from pH 6-9. pH > 9 was not considered since its optimal potential window was close to the oxygen reduction potential,[57, 58] evidenced by unstable baseline currents at pH 10 (see supplementary material Figure S1). For each combination of potential and pH, the PHOH and buffer current response were measured, with results given in Figure 4, respectively.

Based on the ratio of the PHOH and buffer photocurrent, it was observed that the sensitivity of the sensor increased with increasing alkalinity of the buffer solution (see Figure 4.A). This elevation was the result of an increasing PHOH photoresponse (Figure 4.B) and decreasing buffer response (Figure 4.C) as a function of pH.

The main contributors to the PHOH photocurrents when varying pH and applied potential are: i) oxidation rate of PHOH due to $^1O_2$ and ii) electrode surface reduction kinetics of oxidized species. The diffusion rate of (oxidized) PHOH, which is predominantly dependent on the size of the molecule, is not impacted by changes in pH and applied potential.[55]

The photocurrent response for PHOH decreased from pH 6 to 7 from -32 nA to -27 nA and increased exponentially towards pH 9 (see Figure 4.B), with -74 nA at pH 9 when -0.14 V was applied. The increase from pH 7 to pH 9 was caused by the oxidation rate by $^1O_2$. At alkaline pH values, phenolate ion (PHO^-) will become increasingly present. As such, PHOH and PHO^- both contribute to the overall oxidation rate where the oxidation rate for PHO^- is nearly 60 times faster than PHOH.[54] Therefore the overall oxidation rate increases towards pH 9 due to a greater contribution of PHO^- ($pK_a = 9.9$)[54] resulting in increased photoresponse at pH 9. The decrease in response from pH 6 to 7, however, was assigned to the reduction kinetics of *p*-BQ to HQ where reduction was faster at pH 6 due to an increased concentration of protons H^+ in solution.[53] The oxidation rate by $^1O_2$ is the same at pH 6 and 7.[54]

In addition to the oxidation of PHOH by $^1O_2$, a secondary pathway involving PHO^- may also lead to oxidized PHOH, contributing to the PHOH photoresponse. In this pathway, electron transfer from the PHO^- to the excited PS occurs, generating phenoxy radicals and reduced PS species.[46, 59] This electron transfer could occur as the photochemical reduction of $F_{64}PcZn$ in ethanol in the absence of air has been described before.[60] Since this pathway becomes more prevalent when the pH ≈ pK_a of PHOH (9.9), it is expected that at pH 9 a limited contribution to the PHOH photoresponse of this specific secondary pathway is expected.

Finally, by the application of more reductive potentials, −0.17 V at pH 9, the PHOH photocurrent increased by 1.4 times on average due to the higher reduction rate of *p*-BQ at the electrode surface and blank values (from buffer solution, Figure 4.B).

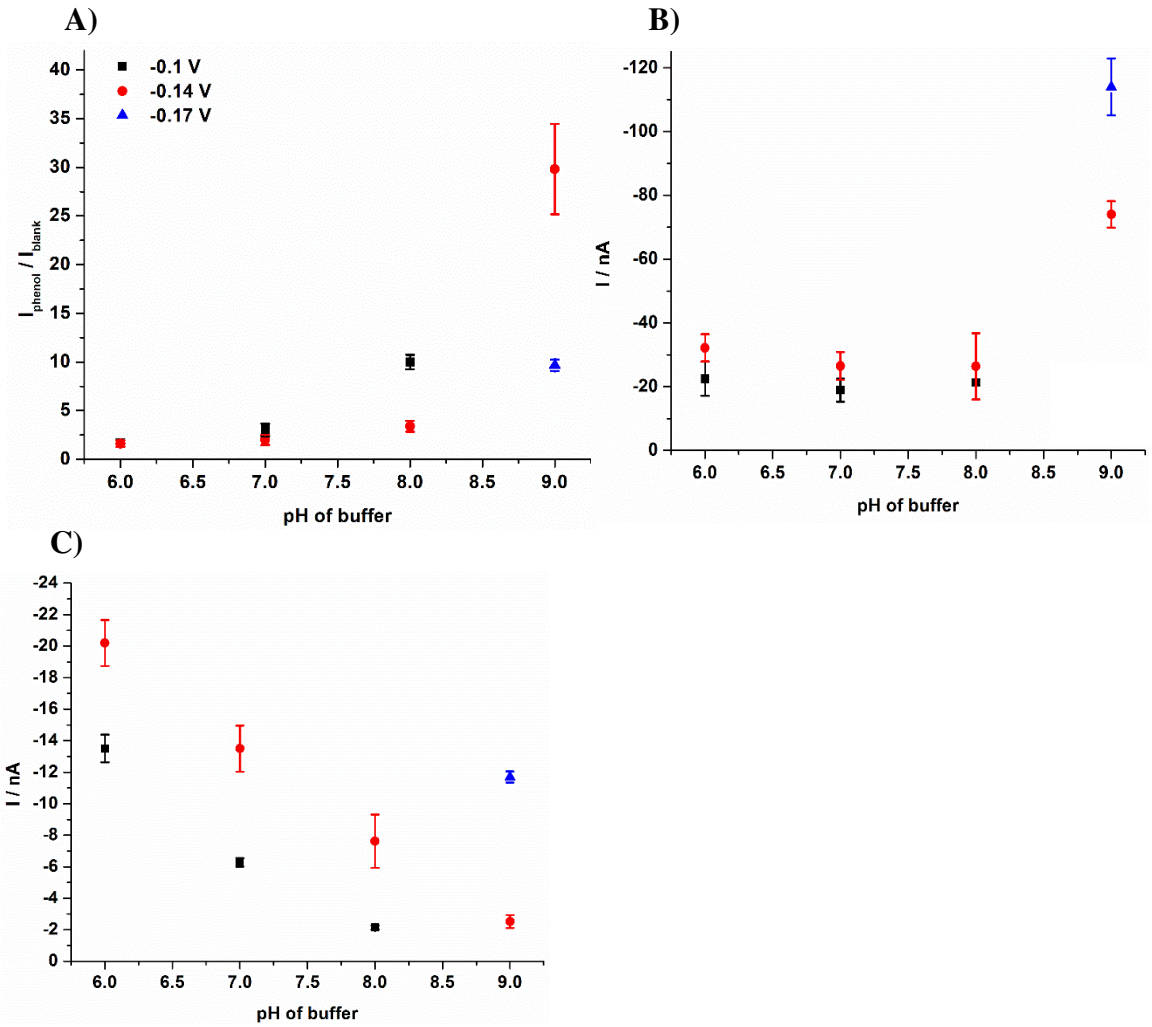

Figure 4. *(A) Ratio of PHOH:buffer photocurrent response as a function of measuring buffer pH. (B) Photocurrent response of 1 µmol L^{-1} PHOH and (C) buffer solution at applied potentials of −0.10 V (black, square), −0.14 V (red, circle) and −0.17 V (blue, triangle) as a function of buffer pH. All potentials are given vs. the Ag pseudo-reference electrode. Error bars denote the standard deviation of three electrodes (N = 3).*

The buffer response is primarily caused by the direct reduction of $^1O_2$ at the electrode surface.[45] Hydroxide is known to quench $^1O_2$,[61] thus, as the pH (and therefore concentration of hydroxide) increases, the quenching of $^1O_2$ becomes more prevalent. As a result, the buffer response decreased as a function of pH (Figure 4.C). A linear trend was observed with a slope of 5.9 ± 0.3 nA per pH unit for −0.14 V and 5.7 ± 0.9 nA per pH unit for −0.10 V *vs.* Ag pseudo-reference electrode (R^2 = 0.99 and 0.95, respectively). Moreover, the use of more reductive potentials, such as

−0.17 V *vs.* Ag pseudo-reference electrode, resulted in elevated blank values most likely due to a higher contribution of generated reactive oxygen species.

In conclusion, based on Figure 4, the optimal conditions for the detection of PHOH were determined as −0.14 V *vs.* Ag pseudo-reference in pH 9 buffer. Using these optimal conditions, a calibration plot for PHOH could be obtained (Figure S2). A sensitivity of 0.45 A mol^{-1} L cm^{-2} and correlation coefficient of 0.99 were computed. The linear dynamic range was 0.05 to 2.00 µmol L^{-1}, with LOD and LOQ of 26 nmol L^{-1} and 88 nmol L^{-1}, respectively, demonstrating the high sensitivity of the sensor compared to other reported electrochemical techniques (Table S1).

Optimized PEC detection of PHOH and other analogues in mixtures. The PEC sensor uses a detection mechanism that interacts with all phenolic compounds in a sample. Since there is a high probability that a company or wastewater sample contains multiple analogues, it is crucial to investigate their contribution to the photoresponse of PHOH. HQ, CC, RC, BPA and the quinone *p*-BQ were selected as phenolic analogues. Their photoresponses were first analyzed individually (Figure 5.A) and then compared when a binary mixture is formed with PHOH (Figure 5.B).

The overall reaction rate with $^1O_2$ consists of a chemical reaction and physical quenching rate. The chemical reaction rate involves a reaction between $^1O_2$ and phenols generating products, e.g. HQ. It is via this reaction pathway that photoresponses are obtained during the PEC measurement. In contrast, no oxidation products are generated during the physical quenching process and thus no photocurrents are expected.[54, 62]

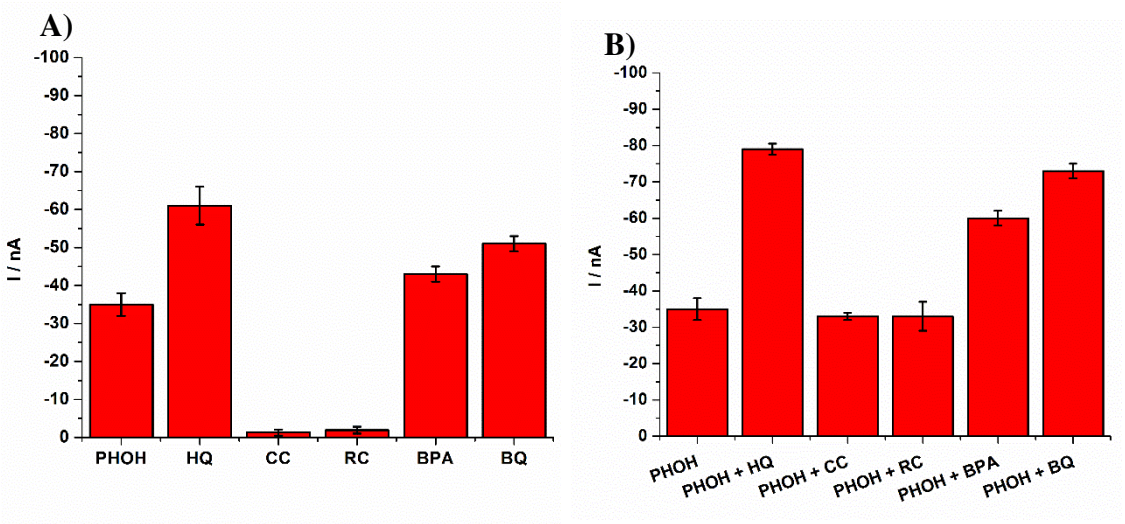

Figure 5. *(A) Photoresponse of 0.5 µmol L^{-1} PHOH, HQ, CC, RC, BPA and p-BQ and (B) their mixtures with PHOH (0.5 µmol L^{-1} + 0.5 µmol L^{-1}) measured in pH 9 buffer at −0.14 V vs. Ag pseudo-reference electrode. Error bars indicate the standard deviation of 18 electrodes (N = 18) for phenol and N = 3 for the remaining species. Blank values were subtracted from the phenolic responses.*

The oxidation of HQ via $^1O_2$ promotes the formation of *p*-BQ while the oxidation of BPA leads to the hydroxylated BPA and cleavage products PHOH, 4-isopropylphenol, HQ and *p*-BQ.[45, 63, 64] Both HQ and BPA exhibit a photocurrent response greater than that for PHOH due to their higher reaction rate with $^1O_2$ (Figure 5.A); approximately 10 times higher in the case of HQ and 3 times higher for BPA (using 4-(1,1-dimethylethyl)phenol as the model compound).[62] However, the addition of HQ or BPA to a PHOH solution led to an increase in the PHOH photosignal (Figure 5.B) which was not equal to the sum of the individual signals. This demonstrates that the phenolic compounds interfere with each other's sensing mechanism/pathway. For instance, the formation of dimers and other polymer structures[38, 65] have a different oxidation rate with $^1O_2$[62] and different redox behavior than the (oxidized) BPA, PHOH or HQ alone.

CC and RC produced almost no photocurrent response (Figure 5.A). CC has a high physical quenching rate[66] with $^1O_2$ so no oxidized products are generated via this pathway. Moreover, a complexation of CC with boric acid (Figure S3), which is a component of the buffer solution, also alters the reactivity with $^1O_2$. The CC-boric acid complex has a higher oxidation potential than CC,[67] consequently reducing its reactivity towards oxidation by $^1O_2$. RC has a relatively high

quantum yield of oxidation by $^1O_2$.[66] However, no photoresponse was detected for RC, likely due to the instability of the *m*-quinone form which rapidly decomposes.[68] Overall, it can be summarized that to obtain high photocurrent responses, the stability of the oxidized products is crucial. As a result, when measuring mixtures of PHOH and its analogues, no increase in photocurrent was detected (Figure 5.B).

Interestingly, the PEC sensor can also measure oxidized phenols. This was demonstrated by the measurement of *p*-BQ (Figure 5.A). The constant application of a reductive potential reduced *p*-BQ to HQ and led to a photosignal when the produced HQ was oxidized by $^1O_2$ during illumination. The obtained signal was greater than for PHOH (Figure 5.A) and resulted in an increase of the PHOH photocurrent when *p*-BQ was added (Figure 5.B). This means that the PEC sensor can even measure oxidized products of phenolic compounds that might be formed during degradation processes.[29, 69]

In conclusion, it is shown that the PEC sensor measures the total contribution of (oxidized) phenolic compounds that generate stable products after oxidation by $^1O_2$. This is a similar working principle as commercially available test kits such as color test kits (with reagent 4-aminoantipyrine)[70] and COD measurements.[47] The latter is not specific to phenols as it measures the total oxidizable organics present in a sample, though it is used by regulatory bodies as an evaluation index of industrial wastewaters.[71] Compared to these test kits, the PEC sensor is highly sensitive and does not require sample preparation, which is advantageous for on-site measurements.[47, 70, 71]

However, based on the photoresponses, the PEC sensor is not able to identify and differentiate between phenols and oxidized phenols. Therefore, to enable this identification feature, a second electrochemical technique, SWV, will be included to identify the phenols based on their oxidation potentials.

Selective SWV sensing of phenolic compounds

Optimization of pH for voltammetric detection of phenols. Voltammetric detection allows the identification and differentiation between structurally related compounds (Figure 1.B) since each phenol has a characteristic electrochemical fingerprint (EF) depending on the pH of the buffer solution, electrode material, among other variables.[48] The electrochemical behavior of PHOH and the selected phenolic analogues was explored at different pH-values on SPEs using

SWV. The EFs of PHOH, HQ, CC, RC and BPA at 20 µmol L^{-1} were obtained in buffers with varying pH values (2, 4, 6, 8, 10 and 12), given in Figure 6. Oxidation peak potentials (E_p) were observed in SWV for all phenols except for BPA. A shoulder is observed for the oxidation peak for BPA at low pHs (pH 2 and pH 4), which was previously reported by Kuramitz *et al.*[72] The E_p at approximately 0 V *vs.* Ag pseudo reference was due to oxidation of silver at the Ag reference electrode.[73]

All phenols showed a shift in oxidation E_p throughout the pH range 2-12 to smaller positive potentials with increasing pH. A linear relationship between the E_p and pH for each phenol is displayed given in Figure S4, with a slope of approximately 60 mV per pH unit, indicating that the number of electrons involved in the oxidation process is equal to the number of protons.[74] The E_p for PHOH at pH 12 deviated from this linearity since the pH > $pK_{a\ (PHOH)}$ (= 9.9).[54] Therefore, PHOH was present in its deprotonated form hence, no proton exchange occurred during the oxidation process. The highest peak separation for the identification between PHOH and its analogues (HQ, CC, RC and BPA) was observed (Figure 6.B, oxidation peak potential of PHOH is denoted by a dotted line) in pH 10 carbonate buffer.[48]

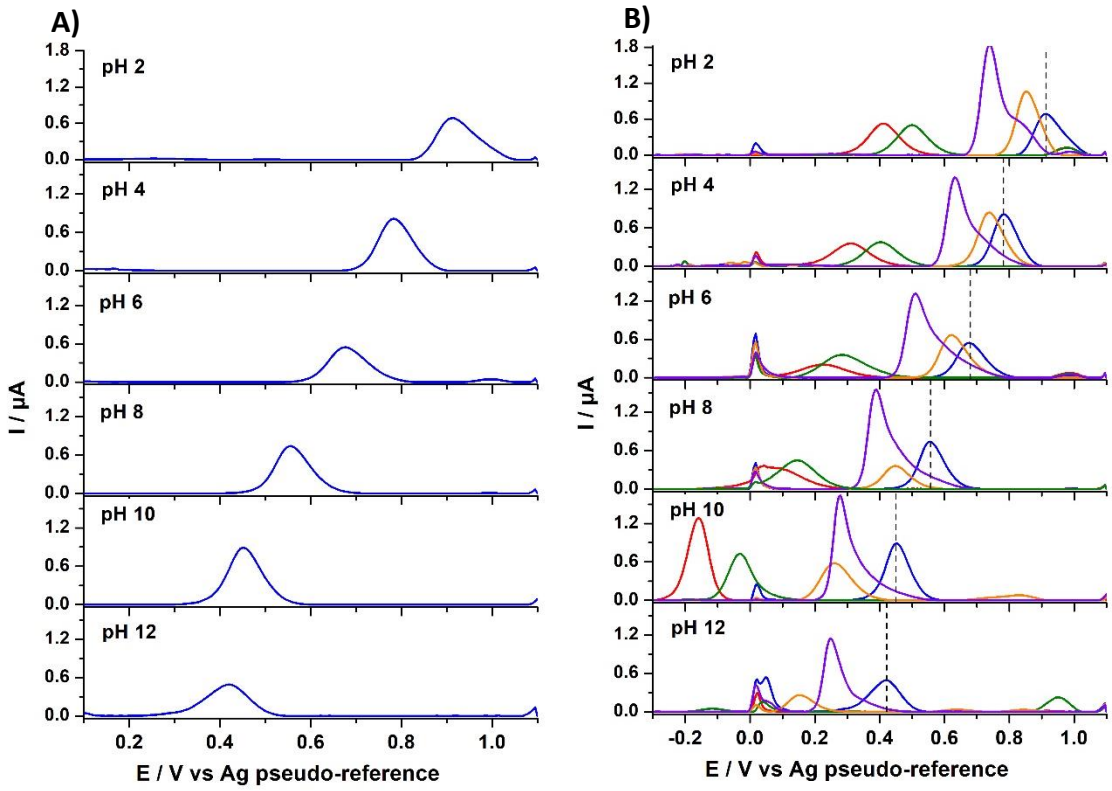

Figure 6. *Baseline corrected square wave voltammograms of (A) 20 µmol L^{-1} PHOH and an overlay of all single phenols (B): PHOH (blue), HQ (red), CC (green), RC (orange) and BPA (purple) measured at different pH values (2, 4, 6, 8, 10 and 12). The dotted line denotes the oxidation peak potential position of PHOH.*

The relationship between oxidation peak current (I_p) and pH was evaluated in order to obtain an optimal current response. Consequently, PHOH, HQ, CC and BPA exhibited the highest I_p intensities (i.e. sensitivity) at pH 10 (Figure S4).

Both HQ and CC did not cause any overlap with PHOH, displaying oxidation peaks at reduced potentials (E_p = −0.15 V and E_p = −0.02 V at pH 10, respectively), which contributed to the oxidation of its corresponding *p*- or *o*-quinone.[29] However, the E_p of both RC and BPA slightly overlapped with the potential region of PHOH. RC exhibited a weak oxidation process at E_p = 0.26 V (at pH 10) and could be the result of the oxidation of hydroxyl groups to a thermodynamically unstable *m*-quinone.[29] Although RC had a similar structure to HQ and CC, it oxidized at a more positive potential. This is likely attributed to the difference in reactivity of these isomers. The aromatic ring of RC has a lower activity since the *meta*-position of the second

hydroxyl group does not activate this ring.[29] Therefore, a larger potential (energy) is required for oxidation. HQ and CC have a higher electron density on both *ortho*- and *para*-positions of the hydroxyl groups, and thus require less energy for oxidation.[29] BPA showed an asymmetric intense oxidation peak at E_p = 0.28 V which overlapped the PHOH oxidation peak (E_p = 0.45 V, pH 10) for all pH values, resulting in a more challenging identification of PHOH.

Consequently, the optimal buffer solution for PHOH confirmation (in complex samples) was pH 10 carbonate buffer where the greatest intensity (and thus sensitivity) for PHOH and elevated differentiation between PHOH and the other phenols was achieved.

Figure S5 shows a calibration curve for PHOH obtained by SWV under optimized conditions with increasing PHOH concentrations (0.25-50.00 µmol L^{-1}). The corresponding linear dynamic range of PHOH was observed between 0.5 to 50.0 µmol L^{-1} with a sensitivity of 0.53 A mol^{-1} L cm^{-2} and a correlation coefficient (R^2) of 0.99. The LOD and LOQ was determined as 0.23 µmol L^{-1} and 0.78 µmol L^{-1}, respectively; showing strong reproducibility of I_p for 20 µmol L^{-1} PHOH with 0.46% RSD, N = 3.

SWV identification of PHOH and other analogues in mixtures. In order to identify PHOH in complex wastewater samples and verify possible peak suppression and/or shift effects under the chosen optimal conditions, binary mixtures were studied. Figure 7 shows the EFs of binary mixtures (ratio of 1:1) for 20 µmol L^{-1} PHOH and 20 µmol L^{-1} of each phenolic compound (HQ, CC, RC and BPA) at the optimal pH 10. The E_p of both phenols in all mixtures could easily be distinguished so that the PHOH oxidation signal was clearly isolated against HQ, CC and RC. A shift of −50 mV and increased intensity of the PHOH peak was observed in the presence of BPA, presumably due to the slight overlap between the oxidation peaks.

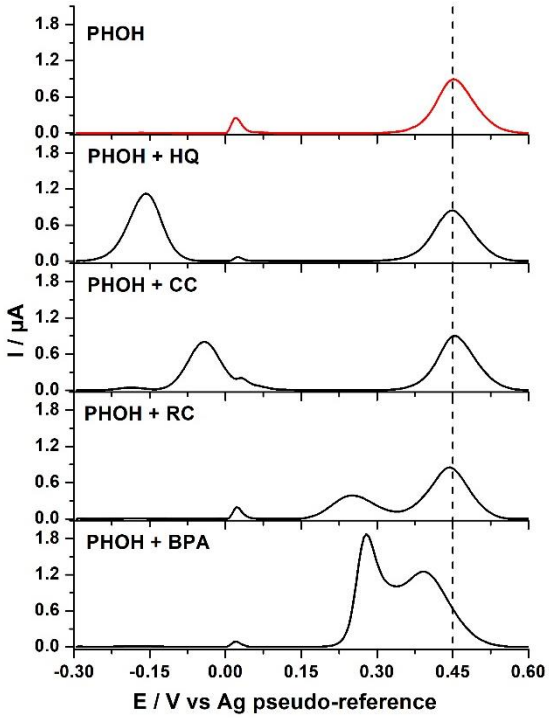

Figure 7. *Baseline corrected square wave voltammograms of 20 µmol L^{-1} PHOH (red, added as reference) and binary mixtures in a 1:1 ratio of 20 µmol L^{-1} PHOH and 20 µmol L^{-1} phenol analogue in pH 10.*

As the primary aim of the combi-electrosensor is the detection of PHOH in the presence of phenolic analogues, the identification of PHOH in complex mixtures (containing HQ, CC, RC and BPA) was studied in pH 10. The oxidation peak of PHOH could be differentiated from HQ, CC and BPA, which makes the chosen conditions suitable for the identification of PHOH (Figure S6). Nonetheless, identification of RC (E_p = 0.26 V) within this complex mixture was not possible as the EF of RC overlaps with the EF of BPA. However, these could be differentiated from the EF of PHOH (Figure 7). The characteristic EF of PHOH is clearly observed in binary and complex mixtures at pH 10 and can be identified from structurally related phenol analogues using SWV on unmodified SPE and without the need for separation techniques.

In conclusion, based on their oxidation potentials, the SWV sensor identifies and distinguishes PHOH from phenol analogues in binary and complex mixtures. Furthermore, the measurement time of the SWV (approximately <5 min) is faster compared to the commercial color kits and COD which is particularly advantageous when measuring multiple samples.[47, 70]

Sensitive PEC and selective SWV sensing of river samples containing phenols

Before the PEC and SWV sensor were combined in a dual sensor set-up, their individual performance was tested by measurements in spiked river samples A-E taken from the Stiemer, Scheldt and Albert Canal (see Table 1). The aim was to determine the phenol concentration, in reference to a PHOH standard, via standard addition by the PEC sensor whilst the SWV sensor identified the phenols in the spiked samples. Five samples were made, each containing 5 µmol L^{-1} PHOH. Additionally, to evaluate a potential matrix effect in the determination of the phenol amount by the PEC sensor. Sample D contained HQ while sample E contained HQ and CC. The initial screening of the river samples via SWV, prior to the spiking of phenols, revealed that almost no electro-active compounds were present (see Figure S7).

The PEC sensor was able to detect phenolic compounds present in the samples. Linearity was obtained upon the addition of PHOH standard (Figure S8). For the spiked river samples containing only PHOH (samples A, B and C), recovery values of 111 ± 8%, 96 ± 9% and 107 ± 12% were calculated, respectively. This indicated that the determined concentrations by the PEC sensor were close to the actual concentration of PHOH in the samples (Table 1) and demonstrates the accuracy of the sensor in these measurements. The repeatability of these measurements was dependent on the performance and reproducibility of the SPE itself and the $F_{64}PcZn|TiO_2$ coatings which were manually deposited. For these sample, the SWV measurements confirmed that only PHOH was present (Figure S9).

When sample D was measured with the PEC sensor, a phenol concentration of 10 ± 1 µmol L^{-1} was computed, while the total added phenolics concentration was 7.5 µmol L^{-1} (Table 1). The greater concentration given by the PEC sensor was a result of the use of a PHOH standard in the standard addition procedure. PHOH has decreased sensitivity than that of HQ and, as a result, the determined total concentration of phenols was higher than 7.5 µmol L^{-1}. Nonetheless, the PEC sensor was able to intercept the addition of HQ in the sample. Furthermore, the SWV sensor could identify HQ and PHOH in this mixture (Figure S10).

In contrast to sample D, the addition of CC to the HQ-PHOH-spiked sample (sample E) did not lead to an increased determined concentration by the PEC sensor. A similar concentration was determined as in the absence of CC (sample D) since CC is photoinactive in these measurement conditions. The SWV sensor detected CC in this sample (Figure S10).

Table 1. *Recorded results of PEC and SWV sensor measurements of spiked river samples. Recorded concentration of phenols by the PEC sensor is expressed relative to the PHOH standard.*

Sample Details		Recorded Results	
		PEC sensor	SWV sensor
Name	Spiked Phenolic Content	C_{PHOH} /µmol L^{-1}	Identified
A	5 µmol L^{-1} PHOH in Stiemer	5.6 ± 0.4	PHOH
B	5 µmol L^{-1} PHOH in Scheldt	4.8 ± 0.5	PHOH
C	5 µmol L^{-1} PHOH in Albert Canal	5.3 ± 0.6	PHOH
D	5 µmol L^{-1} PHOH and 2.5 µmol L^{-1} HQ in Albert Canal	10 ± 1	PHOH and HQ
E	5 µmol L^{-1} PHOH, 2.5 µmol L^{-1} HQ and 10 µmol L^{-1} CC in Albert Canal	11 ± 2	PHOH, HQ and CC

The measurement of multiple phenolic compounds displayed the effectiveness and practicality of the combination of the PEC and SWV sensors showing how each technique improves performance by overcoming limitations these techniques exhibit independently. Furthermore, if one suspects that CC and/or RC are/is present in a sample, SWV measurements are required since CC and RC are photoinactive in the optimal measurement conditions outlined previously. However, an important constraint on the PEC sensor involves the solubility of PS in organic solvents, for instance acetone,[45, 60] which is a byproduct in the production of PHOH via the cumene hydroperoxide route.[1] The performance of the PEC sensor can be compromised when the acetone levels are higher than 20% (Figure S11) due to removal of PSs from the electrode surface and physical destruction of the coating. Therefore, the direct detection of PHOH in highly concentrated acetone streams is currently outside the application range of the PEC sensor. Nevertheless, diluting these concentrated acetone samples will improve the applicability of the PEC sensor.

A combi-electrosensor for the sensitive and selective detection of phenolic compounds

A test combining the PEC and SWV sensor, using one SPE containing two WEs with shared RE and CE (Figure 1A), was performed (Figure 8). Only alkaline pH-values were considered in line with strong sensitivity obtained during the PEC measurements and optimal differentiation via SWV.

Figure 8 displays how the addition of PHOH led to a clear signal (reduction currents) which can be distinguished from the blank value. An increased photocurrent for phenol was observed from pH 8 to 9 due to the higher oxidation rate with $^1O_2$. This was accompanied by a decreasing blank value stemming from an elevated amount of hydroxide at pH 9 and higher quenching rate of $^1O_2$ (Figure 8.A and B).[61] At pH 10, an oxidative blank response and reduced photoresponse for phenol was observed (Figure 8.C). The increased hydroxide concentration at pH 10 will likely increase the quenching rate of $^1O_2$ leading to reduced phenol photosignals and oxidative blank responses.[61] For the SWV measurement, the increase in pH resulted in a shift in PHOH oxidation peaks towards smaller positive potentials (Figure 8.D), as it was described before.

It is important to highlight here that although both sensors have a different optimal pH in the measurement of real samples, this initial test highlights the potential in combining the two techniques on the same SPE. Future steps will pursue the implementation of both techniques on one set-up keeping in mind their different measurement conditions. For this, different SPE configurations can be employed; for instance, i) an array set-up where each sensor has its own three electrode system and measurement condition, ii) a sensor where the RE and CE are shared with two separate WEs or iii) a sensor where the SWV measurement will take place on the same coated WE as the PEC measurement. With the latter configuration being the most challenging one, a deeper optimization should be carried out due to the increased SWV baseline signal caused by the $F_{64}PcZn|TiO_2$-coating on the WE.

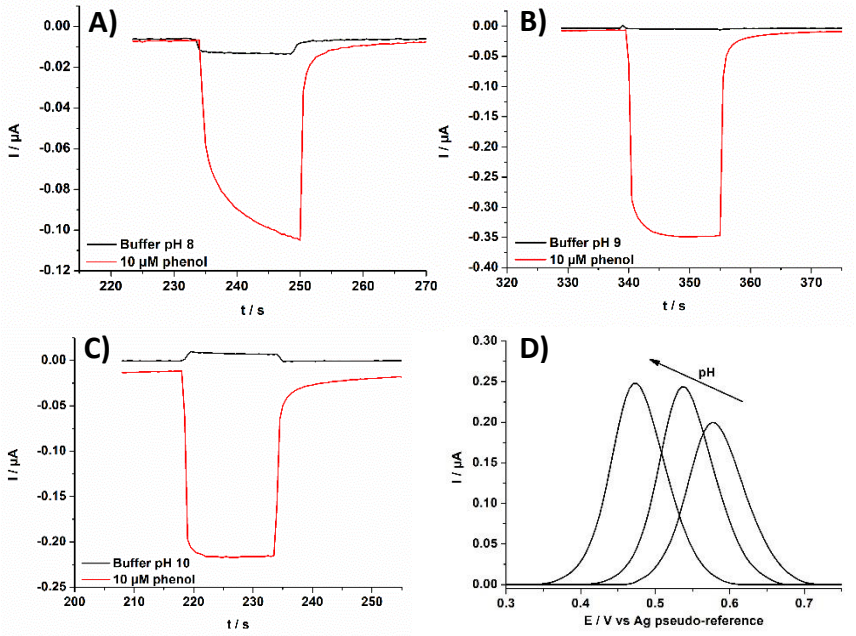

Figure 8. *Photoelectrochemical response measured by the combi-electrosensor at(A) pH 8, (B) 9 and (C) 10 in the presence and absence of 10 µmol L^{-1} PHOH. (D) Baseline corrected square wave voltammetric response of 10 µmol L^{-1} PHOH at pH 8, 9 and 10.*

Conclusions

The effective and practical combination of PEC and SWV for the development of on-site phenol sensors was demonstrated for the first time. Initially, the optimization of the PEC sensor revealed an optimal potential of −0.14 V *vs*. Ag pseudo-reference electrode in combination with pH 9 buffer for the detection of PHOH. Under these conditions, an LOD of 26 nmol L^{-1} was determined, demonstrating the high sensitivity of the sensor. Afterwards, for SWV, an ideal pH 10 was determined for the optimal differentiation between PHOH, BPA, HQ, CC and RC. Using this pH, a PHOH LOD of 0.23 µmol L^{-1} was achieved. Subsequently, via the PEC sensor, the concentration of PHOH in the spiked river samples was measured with a recovery between 96% and 111%. The addition of HQ to the PHOH sample led to an overestimation of the concentration of PHOH which was elucidated by the identification of other phenolic analogues via SWV. However, no photoelectrochemical response was observed for CC and RC, likely due to physical quenching and formation of a boric acid-CC complex, and instability of the oxidized compound of RC. This work demonstrates that the combination of the two techniques (SWV and PEC)

overcomes the photoelectrochemical limitations in terms of selectivity whilst maintaining its advantages. The initial exhibited tests of the combi-electrosensor showed strong potential towards phenolic compound detection in spiked real samples. Further development and optimization will lead to a valuable tool for the on-site detection of phenolic analogues in a wide variety of real samples.

Acknowledgements

FWO is acknowledged for financial support to L.N., H.B. and N.S. (grant numbers 1S09518N, 1SA5620N and 1257922N, respectively). R.C. would like to acknowledge the funding received from the European Union's Horizon 2020 research and innovation program under the Marie Skłodowska-Curie grant agreement No 101024231. The Centre for Functional Materials of Seton Hall University (USA) is thanked for the supported perfluorinated photosensitizer (Prof. Dr. Sergiu M. Gorun). Dr. Amelia R. Langley is thanked for proofreading the manuscript.

Authors contributions

The manuscript was written through contributions of all authors.

Liselotte Neven: Conceptualization; Data curation; Formal analysis; Investigation; Methodology; Validation; Visualization; Roles/Writing - original draft. **Hanan Barich**: Conceptualization; Data curation; Formal analysis; Investigation; Methodology; Validation; Visualization; Roles/Writing - original draft. **Nick Sleegers**: Conceptualization; Data curation; Formal analysis; Investigation; Methodology; Validation; Visualization; Roles/Writing - original draft. **Rocío Cánovas**: Writing - review & editing. **Gianni Debruyne**: Data curation; Formal analysis. **Karolien De Wael**: Conceptualization; Funding acquisition; Project administration; Resources; Supervision; Validation; Visualization; Writing - review & editing.

References

1. Schmidt, R. J., Industrial catalytic processes - phenol production. *Appl Catal a-Gen* **2005,** *280* (1), 89-103.
2. Peng, X. Z.; Yu, Y. J.; Tang, C. M.; Tan, J. H.; Huang, Q. X.; Wang, Z. D., Occurrence of steroid estrogens, endocrine-disrupting phenols, and acid pharmaceutical residues in urban riverine water of the Pearl River Delta, South China. *Sci Total Environ* **2008,** *397* (1-3), 158-166.

3. Chaara, D.; Pavlovic, I.; Bruna, F.; Ulibarri, M. A.; Draoui, K.; Barriga, C., Removal of nitrophenol pesticides from aqueous solutions by layered double hydroxides and their calcined products. *Appl Clay Sci* **2010,** *50* (3), 292-298.
4. Zhou, F. R.; Li, X. J.; Zeng, Z. R., Determination of phenolic compounds in wastewater samples using a novel fiber by solid-phase microextraction coupled to gas chromatography. *Anal Chim Acta* **2005,** *538* (1-2), 63-70.
5. Bolong, N.; Ismail, A. F.; Salim, M. R.; Matsuura, T., A review of the effects of emerging contaminants in wastewater and options for their removal. *Desalination* **2009,** *239* (1-3), 229-246.
6. Kujawski, W.; Warszawski, A.; Ratajczak, W.; Porebski, T.; Capala, W.; Ostrowska, I., Removal of phenol from wastewater by different separation techniques. *Desalination* **2004,** *163* (1-3), 287-296.
7. Veeresh, G. S.; Kumar, P.; Mehrotra, I., Treatment of phenol and cresols in upflow anaerobic sludge blanket (UASB) process: a review. *Water Res* **2005,** *39* (1), 154-170.
8. Lee, H. B.; Peart, T. E.; Svoboda, M. L., Determination of endocrine-disrupting phenols, acidic pharmaceuticals, and personal-care products in sewage by solid-phase extraction and gas chromatography-mass spectrometry. *J Chromatogr A* **2005,** *1094* (1-2), 122-129.
9. Ahmed, S.; Rasul, M. G.; Martens, W. N.; Brown, R.; Hashib, M. A., Heterogeneous photocatalytic degradation of phenols in wastewater: A review on current status and developments. *Desalination* **2010,** *261* (1-2), 3-18.
10. Rahman, M. M.; Alam, M. M.; Asiri, A. M., Development of an efficient phenolic sensor based on facile Ag_2O/Sb_2O_3 nanoparticles for environmental safety. *Nanoscale Adv* **2019,** *1* (2), 696-705.
11. Kuch, H. M.; Ballschmiter, K., Determination of endocrine-disrupting phenolic compounds and estrogens in surface and drinking water by HRGC-(NCI)-MS in the picogram per liter range. *Environ Sci Technol* **2001,** *35* (15), 3201-3206.
12. Meng, J. R.; Shi, C. Y.; Wei, B. W.; Yu, W. J.; Deng, C. H.; Zhang, X. M., Preparation of Fe_3O_4@C@PANI magnetic microspheres for the extraction and analysis of phenolic compounds in water samples by gas chromatography-mass spectrometry. *J Chromatogr A* **2011,** *1218* (20), 2841-2847.
13. Wang, C. J.; Zuo, Y. G., Ultrasound-assisted hydrolysis and gas chromatography-mass spectrometric determination of phenolic compounds in cranberry products. *Food Chem* **2011,** *128* (2), 562-568.
14. Samaras, V.; Thomaidis, N.; Stasinakis, A.; Lekkas, T., An analytical method for the simultaneous trace determination of acidic pharmaceuticals and phenolic endocrine disrupting chemicals in wastewater and sewage sludge by gas chromatography-mass spectrometry. *Anal Bioanal Chem* **2011,** *399* (7), 2549-2561.
15. Ko, E. J.; Kim, K. W.; Kang, S. Y.; Kim, S. D.; Bang, S. B.; Hamm, S. Y.; Kim, D. W., Monitoring of environmental phenolic endocrine disrupting compounds in treatment effluents and river waters, Korea. *Talanta* **2007,** *73* (4), 674-683.
16. Kotowska, U.; Kapelewska, J.; Sturgulewska, J., Determination of phenols and pharmaceuticals in municipal wastewaters from Polish treatment plants by ultrasound-assisted emulsification-microextraction followed by GC-MS. *Environ Sci Pollut R* **2014,** *21* (1), 660-673.
17. Pietrogrande, M. C.; Basaglia, G., GC-MS analytical methods for the determination of personal-care products in water matrices. *Trac-Trend Anal Chem* **2007,** *26* (11), 1086-1094.
18. Campbell, C. G.; Borglin, S. E.; Green, F. B.; Grayson, A.; Wozei, E.; Stringfellow, W. T., Biologically directed environmental monitoring, fate, and transport of estrogenic endocrine disrupting compounds in water: A review. *Chemosphere* **2006,** *65* (8), 1265-1280.
19. Opeolu, B. O.; Fatoki, O. S.; Odendaal, J., Development of a solid-phase extraction method followed by HPLC-UV detection for the determination of phenols in water. *Int J Phys Sci* **2010,** *5* (5), 576-581.

20. Bae, I. K.; Ham, H. M.; Jeong, M. H.; Kim, D. H.; Kim, H. J., Simultaneous determination of 15 phenolic compounds and caffeine in teas and mate using RP-HPLC/UV detection: Method development and optimization of extraction process. *Food Chem* **2015,** *172*, 469-475.
21. Chao, Y. Y.; Tu, Y. M.; Jian, Z. X.; Wang, H. W.; Huang, Y. L., Direct determination of chlorophenols in water samples through ultrasound-assisted hollow fiber liquid-liquid-liquid microextraction on-line coupled with high-performance liquid chromatography. *J Chromatogr A* **2013,** *1271*, 41-49.
22. Alcudia-Leon, M. C.; Lucena, R.; Cardenas, S.; Valcarcel, M., Determination of phenols in waters by stir membrane liquid-liquid-liquid microextraction coupled to liquid chromatography with ultraviolet detection. *J Chromatogr A* **2011,** *1218* (16), 2176-2181.
23. Saraji, M.; Marzban, M., Determination of 11 priority pollutant phenols in wastewater using dispersive liquid-liquid microextraction followed by high-performance liquid chromatography-diode-array detection. *Anal Bioanal Chem* **2010,** *396* (7), 2685-2693.
24. Galceran, M. T.; Jauregui, O., Determination of Phenols in Sea-Water by Liquid-Chromatography with Electrochemical Detection after Enrichment by Using Solid-Phase Extraction Cartridges and Disks. *Anal Chim Acta* **1995,** *304* (1), 75-84.
25. Sun, D.; Zhang, H. J., Electrochemical determination of 2-chlorophenol using an acetylene black film modified glassy carbon electrode. *Water Res* **2006,** *40* (16), 3069-3074.
26. Belkhamssa, N.; da Costa, J. P.; Justino, C. I. L.; Santos, P. S. M.; Cardoso, S.; Duarte, A. C.; Rocha-Santos, T.; Ksibi, M., Development of an electrochemical biosensor for alkylphenol detection. *Talanta* **2016,** *158*, 30-34.
27. Wei, M. C.; Tian, D.; Liu, S.; Zheng, X. L.; Duan, S.; Zhou, C. L., beta-Cyclodextrin functionalized graphene material: A novel electrochemical sensor for simultaneous determination of 2-chlorophenol and 3-chlorophenol. *Sens Actuators B Chem* **2014,** *195*, 452-458.
28. Talarico, D.; Arduini, F.; Constantino, A.; Del Carlo, M.; Compagnone, D.; Moscone, D.; Palleschi, G., Carbon black as successful screen-printed electrode modifier for phenolic compound detection. *Electrochem Commun* **2015,** *60*, 78-82.
29. Enache, T. A.; Oliveira-Brett, A. M., Phenol and para-substituted phenols electrochemical oxidation pathways. *J Electroanal Chem* **2011,** *655* (1), 9-16.
30. Lakshmi, D.; Bossi, A.; Whitcombe, M. J.; Chianella, I.; Fowler, S. A.; Subrahmanyam, S.; Piletska, E. V.; Piletsky, S. A., Electrochemical Sensor for Catechol and Dopamine Based on a Catalytic Molecularly Imprinted Polymer-Conducting Polymer Hybrid Recognition Element. *Anal Chem* **2009,** *81* (9), 3576-3584.
31. Tashkhourian, J.; Daneshi, M.; Nami-Ana, F.; Behbahani, M.; Bagheri, A., Simultaneous determination of hydroquinone and catechol at gold nanoparticles mesoporous silica modified carbon paste electrode. *J Hazard Mater* **2016,** *318*, 117-124.
32. Freitas, J. M.; Wachter, N.; Rocha, R. C., Determination of bisphenol S, simultaneously to bisphenol A in different water matrices or solely in electrolyzed solutions, using a cathodically pretreated boron-doped diamond electrode. *Talanta* **2020,** *217*, 1-9.
33. Yin, H. S.; Zhang, Q. M.; Zhou, Y. L.; Ma, Q. A.; Liu, T.; Zhu, L. S.; Ai, S. Y., Electrochemical behavior of catechol, resorcinol and hydroquinone at graphene-chitosan composite film modified glassy carbon electrode and their simultaneous determination in water samples. *Electrochim Acta* **2011,** *56* (6), 2748-2753.
34. Tan, F.; Cong, L. C.; Li, X. N.; Zhao, Q.; Zhao, H. X.; Quan, X.; Chen, J. W., An electrochemical sensor based on molecularly imprinted polypyrrole/graphene quantum dots composite for detection of bisphenol A in water samples. *Sens Actuators B Chem* **2016,** *233*, 599-606.

35. Wang, J.; Deo, R. P.; Musameh, M., Stable and sensitive electrochemical detection of phenolic compounds at carbon nanotube modified glassy carbon electrodes. *Electroanal* **2003,** *15* (23-24), 1830-1834.
36. Tsai, Y. C.; Chiu, C. C., Amperometric biosensors based on multiwalled carbon nanotube-Nafion-tyrosinase nanobiocomposites for the determination of phenolic compounds. *Sens Actuators B Chem* **2007,** *125* (1), 10-16.
37. Wang, J.; Martinez, T.; Yaniv, D. R.; Mccormick, L. D., Scanning Tunneling Microscopic Investigation of Surface Fouling of Glassy-Carbon Surfaces Due to Phenol Oxidation. *J Electroanal Chem* **1991,** *313* (1-2), 129-140.
38. Yang, X.; Kirsch, J.; Fergus, J.; Simonian, A., Modeling analysis of electrode fouling during electrolysis of phenolic compounds. *Electrochim Acta* **2013,** *94*, 259-268.
39. Rodriguez-Delgado, M. M.; Aleman-Nava, G. S.; Rodriguez-Delgado, J. M.; Dieck-Assad, G.; Martinez-Chapa, S. O.; Barcelo, D.; Parra, R., Laccase-based biosensors for detection of phenolic compounds. *TrAc* **2015,** *74*, 21-45.
40. Rahemi, V.; Trashin, S.; Hafideddine, Z.; Meynen, V.; Van Doorslaer, S.; De Wael, K., Enzymatic sensor for phenols based on titanium dioxide generating surface confined ROS after treatment with H_2O_2. *Sens Actuators B Chem* **2019,** *283*, 343-348.
41. Zhang, Y.; Zhang, J. L.; Wu, H. X.; Guo, S. W.; Zhang, J. Y., Glass carbon electrode modified with horseradish peroxidase immobilized on partially reduced graphene oxide for detecting phenolic compounds. *J Electroanal Chem* **2012,** *681*, 49-55.
42. Mello, L. D.; Sotomayor, M. D. P. T.; Kubota, L. T., HRP-based amperometric biosensor for the polyphenols determination in vegetables extract. *Sens Actuators B Chem* **2003,** *96* (3), 636-645.
43. Wang, Y.; Zhai, F. G.; Hasebe, Y.; Jia, H. M.; Zhang, Z. Q., A highly sensitive electrochemical biosensor for phenol derivatives using a graphene oxide-modified tyrosinase electrode. *Bioelectrochemistry* **2018,** *122*, 174-182.
44. Camargo, E. R.; Baccarin, M.; Raymundo-Pereira, P. A.; Campos, A. M.; Oliveira, G. G.; Fatibello, O.; Oliveira, O. N.; Janegitz, B. C., Electrochemical biosensor made with tyrosinase immobilized in a matrix of nanodiamonds and potato starch for detecting phenolic compounds. *Anal Chim Acta* **2018,** *1034*, 137-143.
45. Trashin, S.; Rahemi, V.; Ramji, K.; Neven, L.; Gorun, S. M.; De Wael, K., Singlet oxygen-based electrosensing by molecular photosensitizers. *Nat Commun* **2017,** *8*.
46. Neven, L.; Shanmugam, S. T.; Rahemi, V.; Trashin, S.; Sleegers, N.; Carrion, E. N.; Gorun, S. M.; De Wael, K., Optimized Photoelectrochemical Detection of Essential Drugs Bearing Phenolic Groups. *Anal Chem* **2019,** *91* (15), 9962-9969.
47. Geerdink, R. B.; van den Hurk, R. S.; Epema, O. J., Chemical oxygen demand: Historical perspectives and future challenges. *Anal Chim Acta* **2017,** *961*, 1-11.
48. Moro, G.; Barich, H.; Driesen, K.; Montiel, N. F.; Neven, L.; Mendonca, C. D.; Shanmugam, S. T.; Daems, E.; De Wael, K., Unlocking the full power of electrochemical fingerprinting for on-site sensing applications. *Anal Bioanal Chem* **2020,** *412* (24), 5955-5968.
49. Chen, H. L.; Yao, J.; Wang, F.; Zhou, Y.; Chen, K.; Zhuang, R. S.; Choi, M. M. F.; Zaray, G., Toxicity of three phenolic compounds and their mixtures on the gram-positive bacteria Bacillus subtilis in the aquatic environment. *Sci Total Environ* **2010,** *408* (5), 1043-1049.
50. Wei, C.; Huang, Q. T.; Hu, S. R.; Zhang, H. Q.; Zhang, W. X.; Wang, Z. M.; Zhu, M. L.; Dai, P. W.; Huang, L. Z., Simultaneous electrochemical determination of hydroquinone, catechol and resorcinol at Nafion/multi-walled carbon nanotubes/carbon dots/multi-walled carbon nanotubes modified glassy carbon electrode. *Electrochim Acta* **2014,** *149*, 237-244.
51. Lohmer, G.; Schnurr, O.; Weber, M.; Weber, M. Process for Treating Phenol. US7,544,845B2, 2009.

52. Al-Nu'airat, J.; Dlugogorski, B. Z.; Gao, X. P.; Zeinali, N.; Skut, J.; Westmoreland, P. R.; Oluwoye, I.; Altarawneh, M., Reaction of phenol with singlet oxygen. *Phys Chem Chem Phys* **2019,** *21* (1), 171-183.
53. Jakobs, R. C. M.; Janssen, L. J. J.; Barendrecht, E., Hydroquinone Oxidation and Para-Benzoquinone Reduction at Polypyrrole and Poly-N-Methylpyrrole Electrodes. *Electrochim Acta* **1985,** *30* (10), 1313-1321.
54. Tratnyek, P. G.; Holgne, J., Oxidation of Substituted Phenols in the Environment - a Qsar Analysis of Rate Constants for Reaction with Singlet Oxygen. *Environ Sci Technol* **1991,** *25* (9), 1596-1604.
55. Blidar, A.; Trashin, S.; Carrion, E. N.; Gorun, S. M.; Cristea, C.; De Wael, K., Enhanced Photoelectrochemical Detection of an Analyte Triggered by Its Concentration by a Singlet Oxygen-Generating Fluoro Photosensitizer. *ACS Sens* **2020,** *5* (11), 3501-3509.
56. Arca, H. C.; Mosquera-Giraldo, L. I.; Pereira, J. M.; Sriranganathan, N.; Taylor, L. S.; Edgar, K. J., Rifampin Stability and Solution Concentration Enhancement Through Amorphous Solid Dispersion in Cellulose omega-Carboxyalkanoate Matrices. *J Pharm Sci* **2018,** *107* (1), 127-138.
57. Kozawa, A.; Zilionis, V. E.; Brodd, R. J., Oxygen and Hydrogen Peroxide Reduction at a Ferric Phthalocyanine-Catalyzed Graphite Electrode. *J Electrochem Soc* **1970,** *117* (12), 1470-&.
58. Lin, C.; Song, Y.; Cao, L. X.; Chen, S. W., Oxygen Reduction Catalyzed by Au-TiO_2 Nanocomposites in Alkaline Media. *ACS Appl Mater Interfaces* **2013,** *5* (24), 13305-13311.
59. Li, C.; Hoffman, M. Z., Oxidation of phenol by singlet oxygen photosensitized by the tris(2,2 '-bipyridine)ruthenium(II) ion. *J Phys Chem A* **2000,** *104* (25), 5998-6002.
60. Moons, H.; Loas, A.; Gorun, S. M.; Van Doorslaer, S., Photoreduction and light-induced triplet-state formation in a single-site fluoroalkylated zinc phthalocyanine. *Dalton Trans* **2014,** *43* (40), 14942-14948.
61. Machado, A. E. H.; Gomes, A. J.; Campos, C. M. F.; Terrones, M. G. H.; Perez, D. S.; Ruggiero, R.; Castellan, A., Photoreactivity of lignin model compounds in the photobleaching of chemical pulps .2. Study of the degradation of 4-hydroxy-3-methoxy-benzaldehyde and two lignin fragments induced by singlet oxygen. *J Photochem Photobiol A: Chem* **1997,** *110* (1), 99-106.
62. Wilkinson, F.; Helman, W. P.; Helman, W. P., Rate Constants for the Decay and Reactions of the Lowest Electronically Excited Singlet State of Molecular Oxygen in Solution. An Expanded and Revised Compilation. *J Phys Chem Ref Data* **1995,** *24* (663).
63. Zhang, T.; Ding, Y. B.; Tang, H. Q., Generation of singlet oxygen over Bi(V)/Bi(III) composite and its use for oxidative degradation of organic pollutants. *Chem Eng J* **2015,** *264*, 681-689.
64. Meng, A. N.; Chaihu, L. X.; Chen, H. H.; Gu, Z. Y., Ultrahigh adsorption and singlet-oxygen mediated degradation for efficient synergetic removal of bisphenol A by a stable zirconium-porphyrin metal-organic framework. *Sci Rep* **2017,** *7*, 1-9.
65. Ferreira, M.; Varela, H.; Torresi, R. M.; Tremiliosi-Filho, G., Electrode passivation caused by polymerization of different phenolic compounds. *Electrochim Acta* **2006,** *52* (2), 434-442.
66. Garcia, N. A., Singlet-Molecular-Oxygen-Mediated Photodegradation of Aquatic Phenolic Pollutants - a Kinetic and Mechanistic Overview. *J Photochem Photobiol B: Biol* **1994,** *22* (3), 185-196.
67. Rafiee, M.; Nematollahi, D., Electrochemical study of catechol-boric acid complexes. *Electrochim Acta* **2008,** *53* (6), 2751-2756.
68. Roithova, J.; Schroder, D.; Schwarz, H., Generation of the elusive meta-benzoquinone in the gas phase. *Angew Chem Int Edit* **2005,** *44* (20), 3092-3096.
69. Trabelsi, F.; AitLyazidi, H.; Ratsimba, B.; Wilhelm, A. M.; Delmas, H.; Fabre, P. L.; Berlan, J., Oxidation of phenol in wastewater by sonoelectrochemistry. *Chem Eng Sci* **1996,** *51* (10), 1857-1865.
70. Zolotov, Y. A.; Ivanov, V. M.; Amelin, V. G., Test methods for extra-laboratory analysis. *TrAC* **2002,** *21* (4), 302-319.

71. Li, J.; Luo, G.; He, L.; Xu, J.; Lyu, J., Analytical Approaches for Determining Chemical Oxygen Demand in Water Bodies: A Review. *Crit Rev Anal Chem* **2018,** *48* (1), 47-65.
72. Kuramitz, H.; Nakata, Y.; Kawasaki, M.; Tanaka, S., Electrochemical oxidation of bisphenol A. Application to the removal of bisphenol A using a carbon fiber electrode. *Chemosphere* **2001,** *45* (1), 37-43.
73. de Jong, M.; Florea, A.; de Vries, A. M.; van Nuijs, A. L. N.; Covaci, A.; Van Durme, F.; Martins, J. C.; Samyn, N.; De Wael, K., Levamisole: a Common Adulterant in Cocaine Street Samples Hindering Electrochemical Detection of Cocaine. *Anal Chem* **2018,** *90* (8), 5290-5297.
74. Brett, C. M. A.; Oliveira-Brett, A. M., Chapter 9: Cyclic Voltammetry and Linear Sweep Techniques. In *Electrochemistry: Principles, Methods and Applications*, Oxford University Press: New York, 1993; pp 174-198.